

Performances of the H-ARQ Adaptive-QAM Transmissions over Multipath Mobile Channels

Vasile Bota, Zsolt A. Polgar, Mihaly Varga

1

Abstract— This paper presents the evaluation of the average spectral efficiencies provided by the adaptive employment of a set of LDPC-coded QAM modulations in an OFDMA downlink scheme over mobile radio channels, assuming a joint channel-access method modeling. It discusses the selection of the set of coded modulations, the setting of the SINR domains where they are optimal and derives the average spectral efficiency provided by this approach in non-ARQ or H-ARQ environments.

Index Terms — LDPC-coded QAM constellations, average spectral efficiency, chunk-error rates, SINR thresholds.

I. INTRODUCTION

THE increase of the average throughput and spectral efficiency of the OFDMA schemes under H-ARQ protocols over mobile radio channels requires a complex approach that involves the following steps: employment of an OFDMA scheme whose parameters are adapted to the channel's coherence time and bandwidth; adaptive employment of coded QAM modulations; selection of powerful high-rate error-control codes; optimal setting of the SINR domains where each coded modulation should be employed; selection of an user-chunk allocation (access) method that should take the best advantage of the channel's frequency and time diversity; modeling the multipath Rayleigh-faded mobile channel. The approach that jointly considers these factors, leads to greater average performances by employing in a better way the channel's time, frequency and multi-user diversity.

The paper studies the spectral efficiency vs. SINR provided by the LDPC-coded QAM modulations adaptively employed in an OFDM downlink transmission scheme governed or not by an H-ARQ protocol with M-chunk packets over mobile multipath Rayleigh-faded channels.

The paper is organized as follows: section II briefly describes the OFDMA transmission scheme used. Section III presents the performance computation of the LDPC-coded QAM modulations employed and considerations regarding the thresholds that separate the SINR domains where each modulation should be used. Section IV briefly describes the joint modeling of the channel and user-access method. Sections V and VI present the computation of the average spectral efficiencies of non-ARQ and H-ARQ transmissions that employ adaptively a set of QAM configurations, LDPC-

coded or non-coded, in the OFDMA scheme. Finally, section VII contains some brief conclusions.

II. OFDMA TRANSMISSION SCHEME

The OFDMA scheme considered [1] has $N_{\text{sbc}}=416$ payload subcarriers; it employs a user-chunk consisting of A subcarriers \times E OFDM-symbol periods ($A=8$, $E=12$) and contains $L=81$ QAM payload symbols, allowing maximum $N_{\text{sbc}}/A=52$ users. For a symbol frequency $f_s=39.0625\text{kHz}$ and a guard-interval $G_T=0.125$, the chunk rate is $C_R=f_s/[(1+G_T)E] = 2983.5\text{ch/s}$, in a bandwidth $BW_{\text{ch}}= A \times f_s = 312.5\text{kHz}$

III. ADAPTIVE CODED QAM MODULATIONS

A. Coded Configurations

A coded configuration is the assembly of an n_t bits/symbol QAM constellation and a LDPC code of rate R_{ct} and N_t bits/codeword. Assuming one codeword/chunk, the configuration rate is $R_{\text{cft}}= N_t/(n_t \cdot L)$, where N_t is the number of information bits/codeword left after shortening the code to match the number of bits available on a L -symbol chunk. t denotes the index of the coded configuration within the set.

This paper employs array-based regular $L2q$ -LDPC codes with a triangular-shaped control matrix and girth equaling 6, as defined in [2]. These codes are defined by parameters (k, j, p) and have $N_t=k \cdot p$ bits, $J_t=(k-j) \cdot p$ information bits and $C_t=j \cdot p$ check bits/codeword. If only coded bits are mapped on the L QAM-symbols of a chunk, the coded configuration rate is:

$$R_{\text{cft}} = 1 - \frac{j \cdot p}{L \cdot n_t} \quad (1)$$

If both coded and non-coded bits are loaded on the n_t -bit QAM symbol, i.e. n_{ct} coded bits, from the N_t bits of the codeword, and n_{nt} non-coded bits (payload bits that are not fed to the LDPC encoder), with $n_t = n_{\text{ct}} + n_{\text{nt}}$, then the coded configuration rate R'_{cft} increases as shown in (2). This approach requires a shorter code with the same coding rate, see also [3].

$$R_{\text{cft}} = 1 - \frac{j \cdot p}{n_t \cdot L} \leq 1 - \frac{j \cdot p}{n_{\text{ct}} \cdot L} = R'_{\text{cft}} \text{ for } n_{\text{ct}} \leq n_t \quad (2)$$

These configurations are decoded with the Message-Passing algorithm (MPA), [4], with maximum $B=15$ iterations/codeword, while the *a posteriori* probabilities of the bits demapped from a QAM symbol are extracted by means of the soft-demapping procedure [5], for both the coded and non-coded bits. The non-coded bits are decided with a soft-decision algorithm that uses the corrected coded bits of the same QAM symbol, [3], as in the Trellis Coded Modulation, [6].

By appropriate use of bit-mapping and demapping and soft-decision algorithm, the error probability of the non-coded bits

¹ Manuscript received January, 31, 2007. This work was partly done in the COST Action 289 "Spectral & Power Efficient Broadband Communications".

All authors are with the Communications Department of the Technical University of Cluj-Napoca, Romania.

Professor V. Bota - email: Vasile.Bota@com.utcluj.ro

Associate-Professor Zsolt A. Polgar - email: Zsolt.Polgar@com.utcluj.ro

Teaching-Assistant Mihaly Varga - e mail: Mihaly.Varga@com.utcluj.ro

is close to the one of the coded bits and so their employment increases the coding rate without affecting significantly the error performances, [3].

Since the chunk duration and bandwidth are chosen to be smaller than the coherence time and bandwidth of the channel, it might be regarded as an AWGN one, defined by the SINR value, during each chunk. Therefore, the set of configurations to be used adaptively will be selected according to their performances on the AWGN channel.

B. Chunk-Error Probability

Considering a set of S configurations, the symbol-error probability p_{et} of a QAM constellation with $W_t (= 2^{n_t})$ points, $t = 1, \dots, S$, and its bit-error rate BER_t are expressed by (3.a) and (3.b), assuming a Gray-mapping of the bits/ symbol, [7].

Because the BER vs. SINR variation of such coded configurations, especially when they map non-coded bits, is not available in literature in a compact analytical form, it was computed by using in (3.a) an equivalent SINR, $SINR_t^{eq}$ (3.c), increased with the coding gain C_{Gt} of the coded configuration t , referred to the non-coded constellation with the same number of bits/symbol. The coding gains were established by computer simulations.

$$p_{et}(SINR_t^{eq}) = \frac{4(\sqrt{W_t} - 1)}{\sqrt{W_t}} Q \left(\sqrt{\frac{3}{(W_t - 1)} \left(\frac{P_s^{eq}}{P_n} \right)_t} \right); \text{ a.} \quad (3)$$

$$BER_t = \frac{p_{et}}{n_t}; \text{ b. } SINR_t^{eq} = SINR_t + C_{Gt} = 10 \lg \left(\frac{P_s^{eq}}{P_n} \right)_t; \text{ c.}$$

The probability of an $L \cdot n_t$ -bit chunk transmitted with configuration t to be correctable received, on a $SINR_t$ -channel, is:

$$p_{ccht}(SNR_t) = (1 - BER_t(SNR_t))^{L \cdot n_t} \quad (4)$$

C. Spectral Efficiency Provided by a Configuration

The nominal bit rate D_{ct} denotes the payload-bit rate that could be reached by the (non)-coded transmission scheme when no post-detection errors occur. The throughput Θ_{ct} denotes the payload-bit rate provided by the correctly decoded chunks on the given channel. Considering the parameters of the OFDMA transmission scheme of section II, the nominal bit rate ensured by a configuration with n_t bits/symbol is:

$$D_{ct} = C_R \cdot L \cdot n_t \cdot R_{cftg} \text{ (bit / s)} \quad (5)$$

The throughput Θ_{ct} (6) is obtained by multiplying the nominal bit-rate to the probability of correctly decoded chunks (4), and the spectral efficiency η_{ct} (7) by dividing Θ_{ct} to the chunk bandwidth BW_{ch} .

$$\Theta_{ct}(SINR_t) = C_R \cdot L \cdot n_t \cdot R_{cftg} \cdot p_{ccht}(SINR_t) \quad (6)$$

$$\eta_{ct}(SINR_t) = \frac{f_s \cdot L \cdot n_t \cdot R_{cftg}}{E \cdot (1 + G_i)} \cdot \frac{1}{A \cdot f_s} \cdot p_{ccht}(SINR_t) \quad (7)$$

For the particular OFDMA scheme of section II it is:

$$\eta_{ct}(SINR_t) = 0.75 \cdot n_t \cdot R_{cftg} \cdot p_{ccht}(SINR_t) \quad (8)$$

D. Selected Set of Coded Configurations

The set of coded modulations to be employed adaptively

should observe the following requirements:

a. each configuration should provide the highest spectral efficiency, out of the members of the set, on a limited domain of SINR; the extension of this domain depends of the SINR range to be covered by the adaptive system and of the number of configurations included;

b. the thresholds separating the configurations' SINR domains might be set by different criteria, in terms of the packet or chunk error-rates accepted by the application;

c. the spectral efficiency variations, between a configuration and its neighbours in the set, should have moderate values of about 0.5- 0.8 bps/Hz; such variations would ensure a smaller granularity of the spectral efficiency, affecting less the average spectral efficiency of the adaptive system when configurations are used outside their domains of optimality, due to erroneous channel estimation/prediction. This requirement calls for a large number of configurations in the set.

Considering the above thumb rules, the set C of $S = 12$ LDPC-coded configurations, built on the 256, 64, 16, 4-QAM and 2-PSK constellations was selected by theoretical computation and computer simulations, see table I.a. The table includes the LDPC code parameters, the configuration rates R_{cftg} , nominal spectral efficiencies, η_{ct} and coding gains C_{Gt} . Their rates and spectral efficiencies are significantly increased by mapping the non-coded bits n_{nt} , besides the coded ones n_{ct} .

A set NC of non-coded modulations composed of 2PSK and 4 to 256-QAM, [8], was considered for reference, table I.b.

TABLE I.a
SET C OF CHUNK CODED CONFIGURATIONS

In de x	Code	n_t	Configuration parameters						
			n_{ct}	n_{nt}	R_{cftg}	η_{ct} [bps/Hz]	T_i [dB]	G_{ci} [dB]	
t	k	j	p	n_{ct}	n_{nt}	R_{cftg}	η_{ct} [bps/Hz]	T_i [dB]	G_{ci} [dB]
0	10	3	17	2	6	0.92	5.52	26.8	4.5
1	15	3	29	4	4	0.86	5.19	25.4	5.5
2	8	4	41	4	4	0.74	4.48	22.8	8.0
3	10	3	17	2	4	0.89	4.02	20.7	4.0
4	12	4	29	4	2	0.76	3.42	17.9	6.5
5	12	4	41	6	0	0.66	2.98	16.4	7.5
6	10	3	17	2	2	0.84	2.52	13.9	5.0
7	9	5	19	2	2	0.84	2.12	12.5	7.0
8	9	4	37	4	0	0.55	1.62	10.1	8.0
9	13	3	13	2	0	0.76	1.13	6.3	4.5
10	8	4	23	2	0	0.43	0.64	3.3	7.5
11	8	3	11	1	0	0.59	0.44	1.9	4.5

TABLE I.b
SET NC OF NON-CODED CONFIGURATIONS

$n_t = n_{nt}$	1	2	3	4	5	6	7	8
----------------	---	---	---	---	---	---	---	---

The spectral efficiencies vs. SINR provided by the configurations of set C are shown in fig. 1.

There should be noted that the spectral efficiency varies slightly, with 0.3-0.5 bps/Hz, between neighboring configurations, thus requiring 12 configurations in the set; also note that DoCoMo uses 14, [9], and Flarion uses 16, [10].

E. Considerations Regarding the Thresholds that Separate the SINR Domains

The paper considers only fixed thresholds, between the SINR domains where each configuration is employed. As

shown in Sec. II. A, the thresholds were established on a fixed AWGN channel. Then, the performances ensured by the set of configurations separated by these thresholds, were evaluated on the desired channel model using a user-chunk allocation (access) method, see section IV.

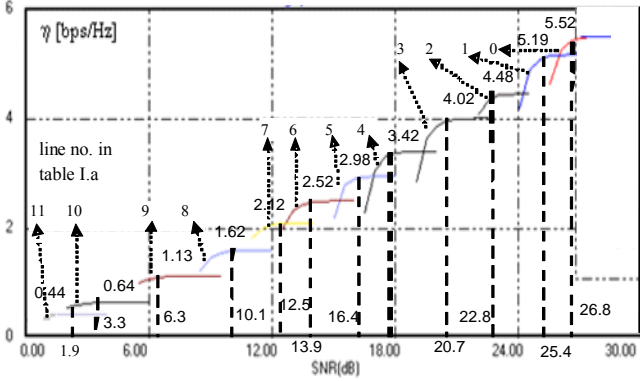


Fig. 1 η_{ek} vs. SINR of configurations of set C , table I.a.

Two criteria were considered for threshold setting:

1. Imposing Chunk-Error Rate $CER \leq 10^{-2}$

The CER vs. SINR curves of set C were derived by computer simulation and the thresholds established accordingly, for the OFDMA scheme of section II. The BER values that ensure $CER=10^{-2}$ range between $2 \cdot 10^{-5}$, for 256-QAM, and $1.2 \cdot 10^{-4}$, for 2-PSK. Table I.a shows the thresholds values T_i .

This constraint ensures a practically constant spectral efficiency for each coded configuration, within its SINR domain, at a value higher than 0.99 of its nominal one, see (7) and (8).

2. Thresholds determined by the intersections of the spectral efficiency curves (CI)

These thresholds take the x-axis values of the intersection points of the $\eta_{ct}(SINR)$ curves of set C , see fig.1. Their values are with 1-1.5 dB smaller than the thresholds obtained by imposing $CER < 10^{-2}$. The spectral efficiencies provided are no longer constant within one SINR interval.

IV. JOINT CHANNEL-ALLOCATION MODELING

The paper considers a 19-paths multipath propagation channel defined by the WP5 Macro model, [11].

The chunk-position that offers the highest SINR during one chunk interval is allocated to each user; this chunk-allocation method [1], [12], called allocation by Best Frequency Position -BFP, employs the channel state prediction, assumed to be perfect, performed by each user for a time-horizon also defined in [1], [12]. The user-chunk and the BFP allocation compose the OFDM-access method.

This channel, together with the set of thresholds presented in Section III and the user-chunk allocation method, i.e. BFP, define an equivalent channel that exhibits S states, i.e. the number of states equals the number of configurations. The states are defined by the thresholds T_i separating the average SINR domains and by the probabilities w_t to be in state St_t , i.e. the average channel SINR to range between T_i and T_{i+1} . A detailed presentation of this joint modeling of the channel and user-chunk allocation method is made in the complementary

paper [13]. The w_t probabilities of the equivalent channel are presented in table II, for a $SINR_0=16$ dB of the firstly-arrived path; the thresholds are the $CER = 10^{-2}$ ones, table I.a. Due to the multipath propagation and to the BFP method, the SINR is greater with 5-10 dB than the $SINR_0$ ensured by the firstly-arrived path during more than 99% of the chunk periods. The SINR does not decrease below 16 dB, due to the BFP access, thus allowing the employment of large QAM constellations with $CER < 10^{-2}$. Therefore, table II contains only the SINR domains greater than 16 dB out of the ones of table I.a.; for the rest of the SINR domains the corresponding w_t have negligible values. For other values of $SINR_0$, the state probabilities w_t are computed with the approximate method presented in [13].

TABLE II
EQUIVALENT-CHANNEL STATE-PROBABILITIES FOR $SINR_0 = 16$ dB

T_i [dB] →	T_5	T_4	T_3	T_2	T_1	T_0	
	16.4	17.9	20.7	22.8	25.4	26.8	
	1	0	$2 \cdot 10^{-4}$	$1.2 \cdot 10^{-3}$	$8.6 \cdot 10^{-5}$	$3.88 \cdot 10^{-2}$	0.9512

V. AVERAGE SPECTRAL EFFICIENCY OF A NON-ARQ SCHEME

The average probability of an M -chunk long packet to be correctible received and the average probability to retransmit such a packet, are expressed by:

$$P_{pc}^{av} = (P_{cch}^{av})^M; \text{ a. } P_R^{av} = 1 - P_{pc}^{av}; \text{ b.} \quad (9)$$

In non-ARQ applications, the nominal average bit rate D_n^{av} , the average throughput Θ_n^{av} and the average spectral efficiency η^{av} are expressed by (10), where R_{cc} denotes the rate of an external correcting code applied to the whole M -chunk packet.

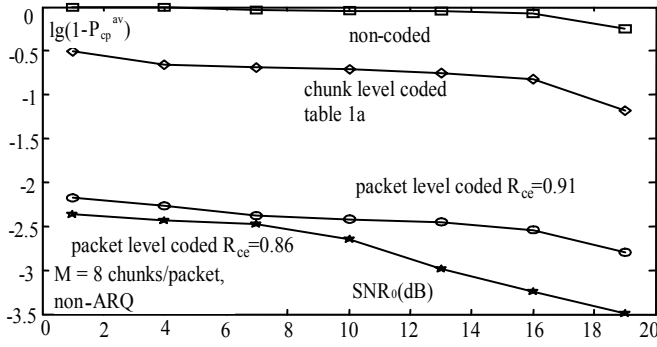
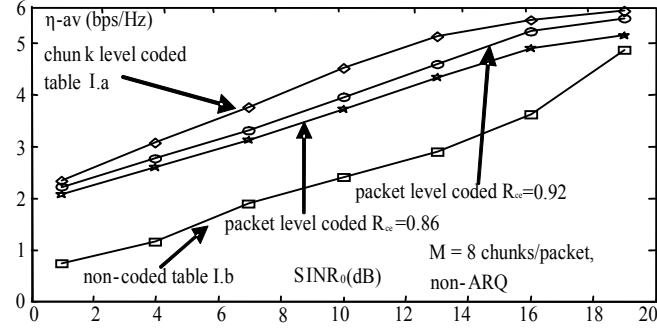
The average time required to transmit a U -bit long frame (U is not an integer multiple of the average chunk length) is computed by (10.d).

$$D_n^{av} = C_R \cdot L \cdot R_{cc} \cdot \sum_{t=1}^S w_t \cdot R_{ct} \cdot n_t; \text{ a. } \Theta_n^{av} = D_n^{av} \cdot P_{cp}^{av}; \text{ b.} \\ \eta^{av} = \frac{\Theta_n^{av}}{BW_{ch}} = \frac{D_n^{av}}{BW_{ch}} \cdot P_{cp}^{av}; \text{ c. } t_n^{av} = \frac{U}{D_n^{av}}; \text{ d.} \quad (10)$$

The packet-error rates and average spectral efficiencies of the adaptive employment of sets C or NC , table I, in the non-ARQ OFDMA scheme, were evaluated, vs. $SINR_0$, on the WP5 Macro channel, $v=70$ km/h, with $M=8$ -chunk packets, for the following coding patterns, see figs. 3 and 4:

- non-coded configurations, using adaptively the NC configurations of table I.b with the $CER \leq 10^{-2}$ thresholds;
- coded configurations at chunk-level, using adaptively the C set of table I.a, with the CI thresholds. i.e. $R_{ct} \neq 1$ and $R_{cc} = 1$;
- non-coded configurations NC ($R_{ct}=1$), used adaptively at chunk-level ($CER \leq 10^{-2}$ thresholds), coded at packet-level with an external LDPC code, $R_{cc}=0.86$, $C_{Ge}=6.5 - 7$ dB;
- same as above, but the external LDPC code has $R_{cc}=0.91$, $C_{Ge}=6 - 6.5$ dB.

The average numbers of bits mapped on a QAM symbol for the coding schemes used are shown in table III, for several values of the $SINR_0$. The table also includes the lengths of the external $R_{cc}=0.86$ codes employed (1 codeword/ packet).

Fig. 3 Packet-error probabilities vs. SINR_0 Fig. 4 Spectral-efficiencies vs. SINR_0

SINR_0 (dB)	n_k^{av} bits/symb C & chunk-coded	n_k^{av} bits/symb NC & ex.-coded	Cwd length 8-chunk/packet
1	4.6243	3.2179	2085
4	5.6974	4.0308	2601
7	6.4736	4.8479	3141
10	7.5527	5.7611	3721
13	7.9677	6.7219	4355
16	7.9975	7.5793	4911
19	8	7.9478	5150

As seen from fig. 3, the packet-error rate ($1 - P_{\text{cp}}^{\text{av}}$) of the chunk-level coding is higher than the one of the packet-level coding. This is due to the employment of the CI thresholds that provide a greater chunk-error rate.

The spectral efficiency of the non-ARQ transmissions is affected by two contradicting factors:

- the average number of bits mapped adaptively/symbol; this number is significantly higher for the chunk-coded scheme, columns 2 and 3 of table III, because the set of configurations is larger and because it maps non-coded bits, increasing the R_{cfg} and the first factor of (10.c);
- the packet-error probability, depending on the packet length, the correction capability of the code and the set of thresholds, which decreases the second factor of (10.c).

The η^{av} is a trade-off between the average n_t (including its granularity and the R_{cfg}) and $P_{\text{cp}}^{\text{av}}$ (depending of C_{Gt} and T_t). Since the value of $P_{\text{cp}}^{\text{av}}$ is limited by the application, it should be set first and the set of configurations that determines the n_t , should be selected accordingly. For the particular case studied, fig. 4 shows that the chunk-coded scheme has higher η^{av} than the packet-coded one, though it exhibits higher packet-error rates. This is because its first factor of (10.c) takes larger values and compensates the smaller value of the second factor.

VI. AVERAGE SPECTRAL EFFICIENCY OF AN - H-ARQ SCHEME

The throughput and spectral efficiency of the OFDMA scheme employing adaptively a set of modulations are now analyzed within a Stop&Wait Hybrid-ARQ (SW H-ARQ) protocol, [14]. The SW-ARQ uses an M-chunk long packet, performing one transmission and q retransmissions of a packet before count time-out. The count timeout lasts for C_T seconds and the protocol resumes the transmission with the packet that generated the time-out. Perfect (N)ACK transmissions across the uplink connection are assumed.

Then, the average probability of a packet to be correctible received and acknowledged after its transmission (first attempt) P_0^{av} , and the average probability of retransmission P_R^{av} are expressed by (11), see also (9).

$$P_0^{\text{av}} = P_{\text{cp}}^{\text{av}}; \text{ a. } P_R^{\text{av}} = 1 - P_0^{\text{av}}; \text{ b.} \quad (11)$$

The average probability P_i^{av} of such a packet to be positively acknowledged after the one transmission and i retransmissions, and the average probability P_T^{av} to reach the count time-out state, i.e. to fail a transmission and q retransmissions, are:

$$P_i^{\text{av}} = (P_R^{\text{av}})^i \cdot P_0^{\text{av}}; \text{ a. } P_T^{\text{av}} = (P_R^{\text{av}})^{q+1}; \text{ b.} \quad (12)$$

The average number of bits that could be transmitted during the time lost in the count time-out state is expressed by a multiple d^{av} of the average packet-length:

$$d^{\text{av}} = \frac{D_n^{\text{av}} \cdot C_T}{M \cdot L \cdot \sum_{t=1}^S n_t \cdot w_t} \quad (13)$$

The average total number N_u^{av} of payload bits that are successfully acknowledged after the (q+1) attempts, is:

$$\begin{aligned} N_u^{\text{av}} &= R_{\text{ec}} \cdot M \cdot L \cdot \left(\sum_{t=1}^S w_t \cdot n_t \cdot R_{\text{ct}} \right) \cdot \sum_{i=0}^q P_0^{\text{av}} (P_R^{\text{av}})^i = \\ &= R_{\text{ec}} \cdot M \cdot L \cdot \left(\sum_{t=1}^S w_t \cdot n_t \cdot R_{\text{ct}} \right) \cdot (1 - (P_R^{\text{av}})^{q+1}); \end{aligned} \quad (14)$$

The second factor of (14) gives the average number of payload bits that are mapped on a QAM symbol. The third factor represents the probability of successful acknowledgement after the i -th retransmission, $i = 0, \dots, q$, and is reduced to a shortened form by using the sum of a geometrical progression.

The average total number, $N_{\text{tot}}^{\text{av}}$, of transmitted bits required to successfully acknowledge the N_u^{av} bits, after the q+1 attempts and including the count time-out, is:

$$\begin{aligned} N_{\text{tot}}^{\text{av}} &= M \cdot L \cdot \left(\sum_{t=1}^S w_t \cdot n_t \right) \cdot \left[\sum_{i=0}^q (i+1) \cdot P_0^{\text{av}} \cdot (P_R^{\text{av}})^i + (q+1) \cdot P_T^{\text{av}} + d^{\text{av}} \cdot P_T^{\text{av}} \right] = \\ &= M \cdot L \cdot \left(\sum_{t=1}^S w_t \cdot n_t \right) \cdot \left[\frac{1 - (P_R^{\text{av}})^{q+1}}{1 - P_R^{\text{av}}} + d^{\text{av}} (P_R^{\text{av}})^{q+1} \right] \end{aligned} \quad (15)$$

The $N_{\text{tot}}^{\text{av}}$ is composed of three terms:

- the average number of bits transmitted to acknowledge the packet in i attempts, $i = 0, \dots, q$ - first two factors multiplied to the first term of the third factor;
- the average number of bits transmitted before reaching the count time-out (q+1 unsuccessful attempts) - first two

factors multiplied to the second term of the third factor;
- the average number of bits that could be transmitted during the count time-out - first two factors multiplied to the third term of the third factor.

The protocol efficiency, i.e. the ratio between the N_u^{av} and the N_{tot}^{av} , is then expressed by (16):

$$\zeta_H = \frac{M \cdot L \cdot R_{cc} \cdot \sum_{t=1}^S w_t \cdot n_t \cdot R_{ct}}{M \cdot L \cdot \sum_{t=1}^S w_t \cdot n_t} \cdot \frac{(1 - P_R^{av}) \cdot (1 - (P_R^{av})^{q+1})}{\left[1 - (P_R^{av})^{q+1} + d^{av} \cdot (P_R^{av})^{q+1} \cdot P_0^{av} \right]} \quad (16)$$

The average throughput and spectral efficiency of the transmission governed by the H-ARQ protocol are, respectively:

$$\Theta_H^{av} = C_R \cdot L \cdot \left(\sum_{t=1}^S w_t \cdot n_t \right) \cdot \zeta_H; \quad a. \quad \eta_H^{av} = \frac{\Theta_H^{av}}{BW_{ch}} \cdot \zeta_H; \quad b. \quad (17)$$

Note that if the protocol requirements are removed, no count time-out ($d^{av}=0$) and no retransmissions ($q=0$), the $\zeta_H = P_{cp}^{av}$, see (13) and (14), and the spectral efficiency is the one of the non-protocol schemes, see (10.c) and (17).

For $q > 0$, the ζ_H is smaller than P_{cp}^{av} and increases with q ; for an infinite number of retransmissions ($q \rightarrow \infty$), the $\zeta_H \rightarrow P_{cp}^{av}$, and the spectral efficiency of the protocol scheme (17) tends to the one of the non-protocol scheme, (10).

The average time required to transmit an M-chunk packet under the H-ARQ protocol is:

$$t_p^{av} = 1 / (C_R \cdot \zeta_H) \quad (18)$$

A U-bit long frame is spread into J packets, (19) and is transmitted, on average, in a time interval equaling $J \cdot t_p^{av}$.

$$J = \left\lceil \frac{U}{\left(M \cdot L \cdot R_{cc} \cdot \sum_{t=1}^S w_t \cdot R_{ct} \cdot n_t \right)} \right\rceil + 1 \quad (19)$$

The two contradictory factors that affect the η^{av} presented in section V, (10.c), also affect η_H^{av} in a similar manner, but P_{cp}^{av} is replaced by the second factor of ζ_H , (16).

The spectral efficiencies vs. $SINR_0$ provided by the sets C and NC of Section III. C, were evaluated in an H-ARQ protocol for the same OFDMA scheme, channel and coding patterns as in section V, see fig. 5. The H-ARQ parameters were: $q=3$, $d^{av}=5$ and $M=8$ chunks/packet.

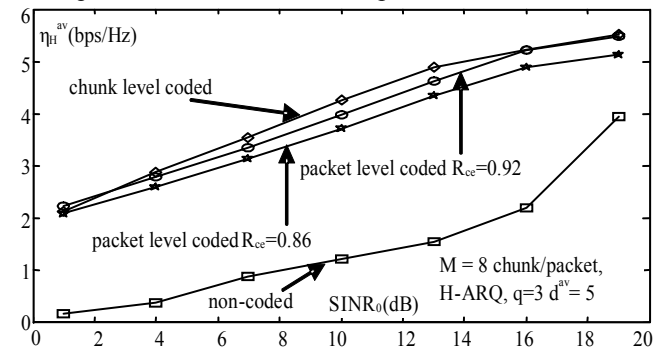


Fig. 5 Average spectral efficiencies vs. $SINR_0$ under H-ARQ

For $M=8$, the chunk-level coded scheme provides a higher spectral efficiency than the packet-level coding schemes, as in the non-protocol scheme, due to the same reasons. For longer packets, the two coding schemes have about the same η_H^{av} .

The values of η_H^{av} are smaller than in the non-protocol case

due to the count time-out interval C_T , d^{av} in (16). The increase of C_T , compared to the packet duration, leads to a significant decrease of the spectral efficiency; it may be compensated by increasing q , at the expense of an increased delay inserted.

VII. CONCLUSIONS

The average spectral efficiency η^{av} of such transmissions is affected by the number of configurations adaptively used for both non-ARQ and H-ARQ schemes. The coding rates of these configurations affect in two contradictory ways the η^{av} : by decreasing the number of payload bits and by increasing their probability of correct decoding. The trade-off between these trends is accomplished within a limited range of SINR, where the respective configuration should be used. The efficiency and the delay of the H-ARQ schemes are also depending of the number of retransmissions. Due to the numerous factors that have contradicting influences, the efficiency provided by such a scheme should be analyzed for each particular case.

For the particular case studied, the chunk-level coding ensures higher spectral efficiencies for small packets, while for long frames (more packets) the two coding patterns provide close spectral efficiencies, in both modes of transmission. This conclusion holds for coding schemes that employ only one correcting code, either at the chunk or at the packet levels.

A significant increase of the average spectral efficiency might be brought by the use of concatenated codes, the outer code at the packet-level and the inner one at the chunk-level. The derivation of the average spectral efficiency proposed in this paper may be applied for such coding schemes, both for non-ARQ and for H-ARQ transmissions, by setting both R_{cc} and R_{ct} to their appropriate values, < 1 , in (10) or (16) and by computing the p_{pcht} , (3) and (4), and P_{cp}^{av} (9) accordingly.

REFERENCES (SELECTED)

- [1] IST-2003-507581 WINNER, "Final report on identified RI key technologies, system concept, and their assessment", Report D2.10 v1.0.
- [2] E. Eleftheriou, S. Olcer, "G.gen:G.dmt.bis:G.lite.bis: Efficient Encoding of LDPC Codes for ADSL", ITU-T, Temporary Document SC-064, 2002.
- [3] V. Bota, Zs. Polgar, M. Varga, "Performances of LDPC-Coded OFDM Transmissions and Applications on Fixed and Mobile Radio Channels", MCM of COST 289 "Spectrum and Power Efficient Broadband Communications", Barcelona, 2004.
- [4] D. J. C. McKay, "Good error-correcting codes based on very sparse matrices," *IEEE Trans. on Information Theory*, vol. 45, March, 1999.
- [5] ITU-T, "LDPC codes for G.dmt.bis and G.lite.bis," Temporary Document CF-060.
- [6] G. Ungerboeck, "Trellis-Coded Modulation with Redundant Signal Sets, Part I, II", *IEEE Communications Magazine*, vol.25, No.2, 1987.
- [7] Th. S. Rappaport, *Wireless Communications*, Prentice Hall PTR, 2001.
- [8] V. Bota, M. Varga, Zs. Polgar, "Convolutional vs. LDPC Coding for Coded Adaptive-QAM Modulations on Mobile Radio Channels", MCM of COST 289, Madrid, 2005.
- [9] H. Atarashi, N. Maeda, S. Abeta, M. Sawahashi - "Broadband Packet Wireless Access Based on VSF-OFCDM and MC/DS-CDMA", *Proc. of PIMRC 2002*.
- [10] R. Dineen, - "Flarion Technologies", Ovum 2004.
- [11] IST-2003-507581 WINNER, "Assessment of Radio-link technologies", Report D2.3 ver 1.0, 2005.
- [12] M. Sternad, T. Ottosson, A. Ahlen, A. Svensson, "Attaining both Coverage and High Spectral Efficiency with Adaptive OFDM Downlinks", *Proc. of VTC 2003*, Orlando, Florida, 2003
- [13] Zs. Polgar, V. Bota, M. Varga, A. Gameiro, "Joint Modeling of the Multipath Radio Channel and User-Access Method", *Proc. of Fourth COST 289 Workshop*, Gothenburg, 2007.
- [14] H. Tanenbaum, *Computer Networks*, Prentice Hall, 1989.